JOURNAL OF MATERIALS SCIENCE 27 (1992) 6797–6806

Effect of heating rate on the combustion synthesis of Ti–Al intermetallic compounds

H. C. YI, A. PETRIC
Department of Materials Science and Engineering, McMaster University, Hamilton, Ontario, Canada L8S 4L7

J. J. MOORE
Department of Metallurgical and Materials Engineering, Colorado School of Mines, Golden, CO 80401, USA

Titanium aluminide compounds were synthesized by the thermal explosion mode of self-propagating high-temperature synthesis (SHS). The effects of heating rate on the combustion characteristics and the microstructures of the products were studied. It was found that the low density of the reacted sample was due to the outgassing of water vapour and other gases, which were released by dissociation of hydrated aluminium oxides. Higher heating rates resulted in a product of higher density and single-phase microstructure. At lower heating rates, the reaction product was a mixture of phases for TiAl and Ti_3Al reactions. A liquid (Al)–solid (Ti) reaction mechanism is predicted for slow heating while a solid–solid mechanism is expected for high heating rates. The origin of porosity in the product is also discussed.

1. Introduction

The titanium aluminides have considerable development potential as high-temperature materials for aircraft due to their refractory nature and low densities. However, they also have very limited ductility at room temperature which makes their processing not viable through the conventional melting–casting route. For this reason, many alternative techniques for producing these compounds have been sought.

One alternative method is self-propagating high-temperature synthesis (SHS), also known as combustion synthesis [1]. There are three intermetallic compounds of interest in the Ti–Al system as shown in Fig. 1 [2]: Ti_3Al, TiAl and $TiAl_3$. Some of the properties are shown in Table I. Of the three compounds, TiAl has been produced by the combustion mode [3–6]. This involves initiating the reaction by rapid heating of one end of the sample. The reaction zone propagates as a wavefront through the sample, driven by the exothermic heat of formation. Table I also shows the adiabatic temperatures (T_{ad}) based on the assumption that the reactions were initiated at 298 K and 933 K (the melting point of aluminium). If the reactions are initiated at 933 K, their adiabatic temperatures will be higher than the melting points of the corresponding compounds but no exact values could be calculated because of the lack of thermodynamic data. Although 298 K is chosen as the ignition temperature for calculation, it is actually impossible to ignite reactions at room temperature and preheating is required. For the Ti + Al = TiAl reaction, preheating the pellet above 373 K was necessary to initiate and sustain a stationary reaction wave. Below 323 K, the reaction front was extinguished [4]. Products produced by the combustion mode were found to be porous. However, hot isostatic pressing has been used successfully to fully densify the TiAl compound [7, 8].

The thermal explosion mode has been found to be more suitable to produce less exothermic intermetallic or metallic systems such as Ni–Al [9], Ti–Ni [10, 11] and Cu–Al [12]. In this mode, the compacted reactant powders are heated up at a constant rate until the reaction is initiated uniformly throughout the pellet. By monitoring the temperature as a function of time during heating, details of the reaction are revealed by peaks on the curve. Progress of the reaction is affected by various parameters, such as stoichiometry, heating rate and reactant particle size. This paper examines the influence of some of these factors in the combustion synthesis of Ti–Al compounds by the thermal explosion model.

2. Experimental procedure

Titanium and aluminium powders of -325 mesh (<45 μm) were used during this investigation. However, sieve analysis results (Table II) show a considerable amount of aluminium powder with particle sizes larger than 45 μm, although it may be due to agglomeration. The powders were mixed in the required stoichiometries and tumbled for 10 min to assure a homogeneous mixture. They were then pressed into cylindrical pellets (ϕ 8 mm) with density around 70 $\pm$ 2% of theoretical (determined by dimension measurement) by uniaxial pressing in a tool-steel die with two plungers. Each pellet weighed between 1 and 2 g.

0022–2461

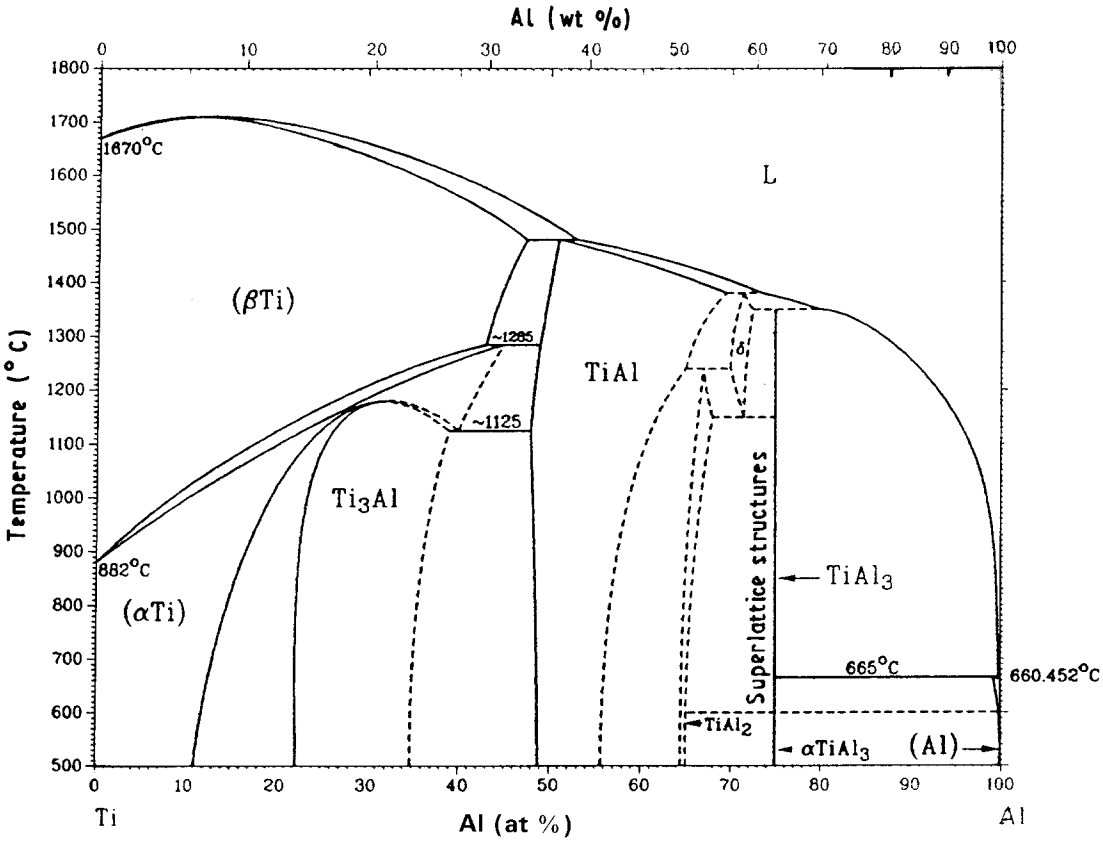

Figure 1 Phase diagram of the Ti–Al system [2].

TABLE I Heat of formation and adiabatic temperature for the three intermetallic compounds in the Ti–Al system

Compound	Density ($g\,cm^{-3}$)	Crystal structure	T_m(K)	$\Delta H^0_{f,298}$ ($kcal\,mol^{-1}$)	T_{ad}(K)	
					$T_0 = 298$ K	$T_0 = 933$ K
Ti_3Al	4.2	$DO_{19}(\alpha_2)$	1873	–	–	–
TiAl	3.9	$L1_0$ (γ)	1733	– 17.4	1518	> 1733
$TiAl_3$	3.4	DO_{22}	1613	– 34.0	1517	> 1613

TABLE II Sieve analysis of aluminium and titanium powders

	Ti[a]	Al[b]
Purity (%)	99	99.8
Particle size distribution (wt %)		
< 38 μm	92.5	34.6
38–45 μm	7.3	8.5
45–53 μm	0.2	6.5
53–75 μm		16.1
75–106 μm		14.3
106–150 μm		10.0
> 150 μm		10.0

[a] Johnson Matthey, Seabrook, New Hampshire.
[b] Alfa Division, Andover, Massachusetts.

A 0.7 mm diameter hole was drilled at one end to accommodate the Pt–Pt13% Rh thermocouple which was made of 0.25 mm wires.

The sample was heated under flowing ultra-high purity argon at a constant heating rate until the reaction between two elements began throughout the sample. The heating was stopped as soon as the reaction was finished and the sample was then allowed to furnace-cool to room temperature. The argon flow rate was set at or below 25 $cm^3\,min^{-1}$. The objective was to investigate the effect of heating rate and aluminium particle size on the combustion characteristics, i.e. ignition (T_{ig}) and combustion (T_c) temperatures, the reaction mechanism as well as the structure of the products. The density of the reacted products was determined by the water displacement method. Microstructures were characterized by X-ray diffraction (XRD), optical and scanning electron microscopy (SEM).

3. Results

Four compositions were studied: Ti–62.8 wt % Al, Ti–40 wt % Al, Ti–27.3 wt % Al and Ti–15.8 wt % Al which correspond to Al_3Ti, AlTi, AlTi + $AlTi_3$ and $AlTi_3$ compounds, respectively. Fig. 2 shows a typical temperature–time curve of reacting a Ti–40 wt % Al

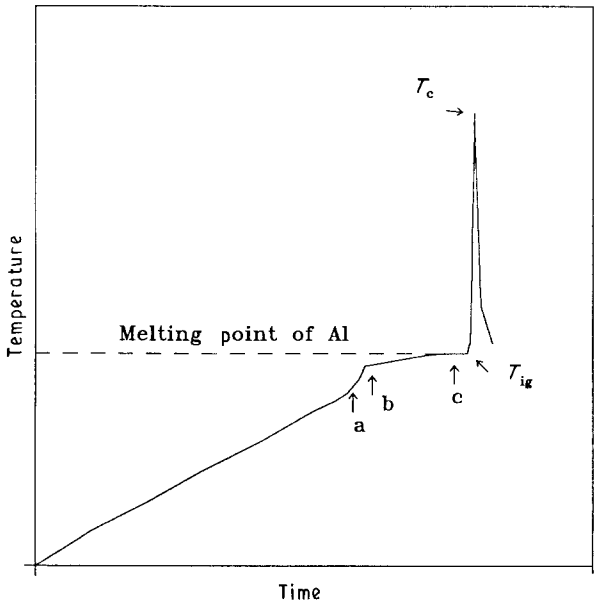

Figure 2 A typical temperature–time recording in the combustion synthesis of TiAl compound.

pellet (AlTi) at a heating rate of 10 K min^{-1}. Two exothermic peaks were recorded. The first peak was initiated at 550 °C (T_{ig}) with a corresponding combustion temperature of 630 °C. The second peak was initiated at the melting point of aluminium and reached a combustion temperature of 1270 °C, which is lower than the adiabatic temperature shown in Table I. The temperature–time profiles for the other three reactions during the heating were similar to Fig. 2.

3.1. Effect of heating rate

Throughout this work, heating rates of greater than 1 K min^{-1} were used since under lower heating rates, the compounds may be formed by diffusion similar to the sintering process. The influence of heating rate on T_{ig} and T_c of both peaks for TiAl reactions is shown in Fig. 3. For the first exothermic peak, the ignition was found to occur in the temperature range 520–570 °C and did not vary with the increase in heating rate. On the other hand, the combustion temperature was slightly below the melting point of aluminium when the heating rate was less than 15 K min^{-1} but appeared to decrease with an increase in heating rate. It was also found that no first peak was recorded when the heating rate was equal to or lower than 2 K min^{-1}. For the second peak, the ignition temperature is around the melting point of aluminium at a heating rate of 10 K min^{-1} or less, indicating that the reaction is associated with liquid aluminium reacting with solid titanium. There is also a clear trend of decreased ignition temperature with increased heating rate, such that ignition of the second peak begins below the melting point of aluminium at a heating rate of 50 K min^{-1}, indicating a solid (Al)–solid (Ti) reaction mechanism. The combustion temperature, which is insensitive to the heating rate as shown in the Fig. 3b,

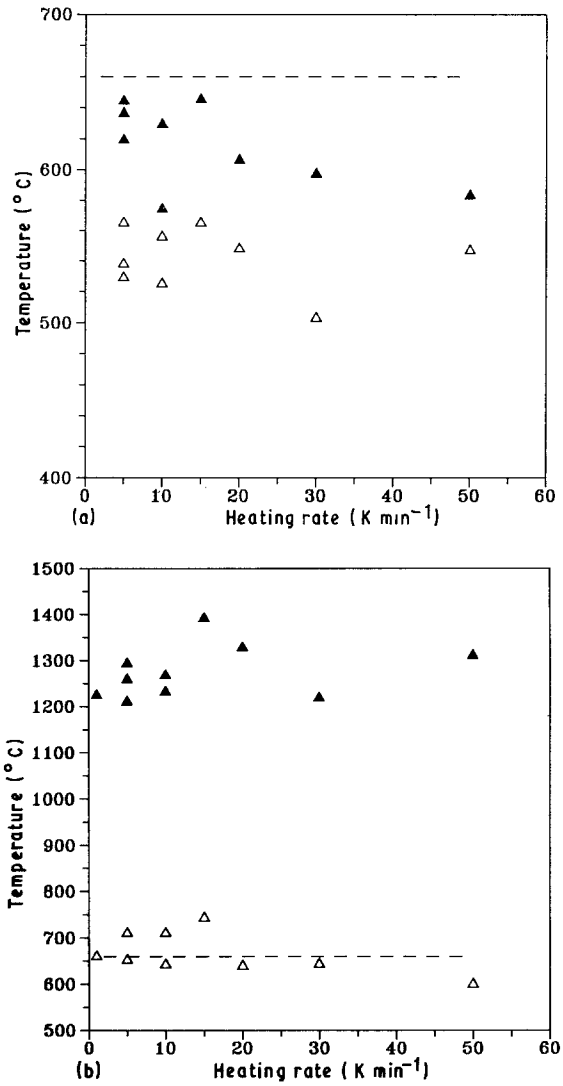

Figure 3 Effect of heating rate on (△) ignition and (▲) combustion temperatures of (a) the first peak and (b) the second peak in the combustion synthesis of the TiAl compound; (– – –) melting point of Al.

is near 1300 °C, lower than the melting point of the TiAl compound and the adiabatic temperature (Table I).

The XRD patterns and the optical microstructures for the TiAl reaction are shown in Figs 4 and 5, respectively, for heating rates of 10 and 50 K min^{-1}. It is very obvious from the two figures that for the 10 K min^{-1} rate, the reacted sample is composed of a mixture of the three intermetallic compounds in the Ti–Al system, whereas for 50 K min^{-1} the reacted product is mainly TiAl phase with only traces of the other phases, mainly Ti_3Al. It was also found that the porosity distribution was more homogeneous for the sample with the 10 K min^{-1} heating rate, whereas for the sample prepared at 50 K min^{-1} there remained a large central void, indicating a more violent reaction.

The heating rate also has a tremendous influence on the apparent density of the products. As shown in Fig. 6, the apparent densities of reacted TiAl samples increased from 48 to 58% as the heating rate increased from 10 to 50 K min^{-1} despite the large void in the

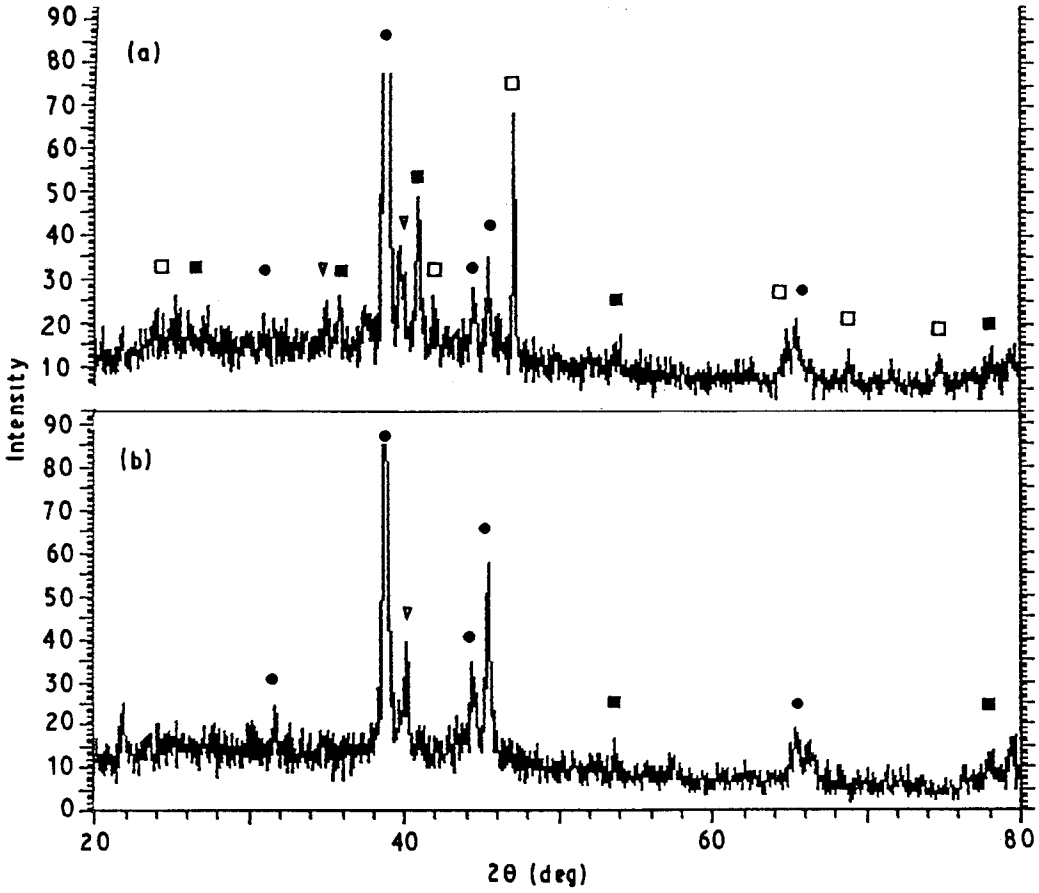

Figure 4 XRD patterns of TiAl product under different heating rates: $\dot{T}$ = (a) 10 and (b) 50 K min^{-1}. (●) TiAl, (□) $TiAl_3$, (■) Ti_3Al, (▽) Ti.

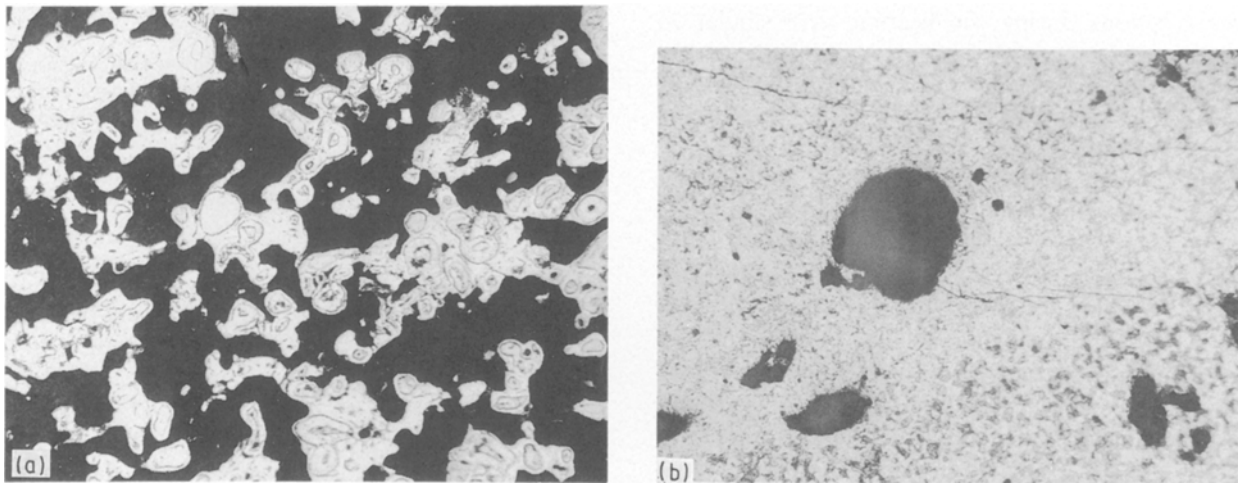

Figure 5 Optical micrographs of the TiAl product under different heating rates: $\dot{T}$ = (a) 10 and (b) 50 K min^{-1} (× 150).

latter sample. It was also found that the density did not change with varying heating rates below 10 K min^{-1}.

Figs 7–12 show the effect of heating rate on T_{ig} and T_c, XRD pattern and microstructure of $TiAl_3$ and Ti_3Al reaction products. As in the case of the TiAl reaction, both T_{ig} and T_c show little change with increase in heating rate for either the Ti_3Al or $TiAl_3$ reaction. But for the $TiAl_3$ reaction, the product was solely $TiAl_3$ phase regardless of the heating rate as can be seen from Fig. 8, whereas for the Ti_3Al reaction, the product also contained a considerable amount of second phase (Fig. 12). The product density of $TiAl_3$ changed more dramatically than that of TiAl as shown in Fig. 13. As the heating rate increased from 2 to 50 K min^{-1}, the density increased from 29 to 58%. Similar to the TiAl reaction, the $TiAl_3$ produced at low heating rate has evenly distributed porosity, and a large central void for high heating rate. In the case of Ti_3Al, there is virtually no change in density under

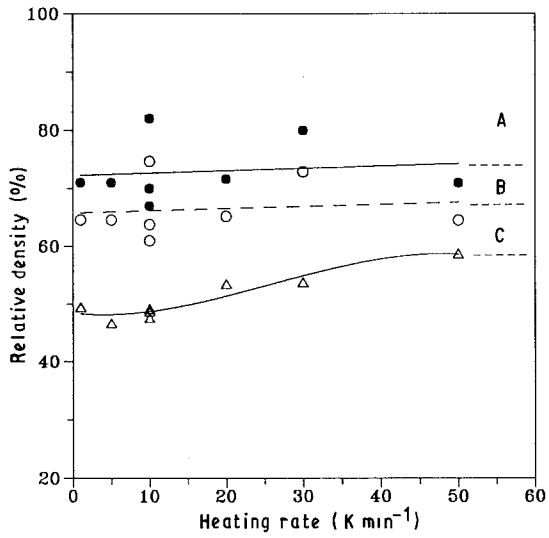

Figure 6 Effect of heating rate on the density changes of Ti + Al = TiAl reaction; regions A, B, C represent three kinds of porosity. (○) 0.911 relative green density, (●) relative green density, (△) relative product density.

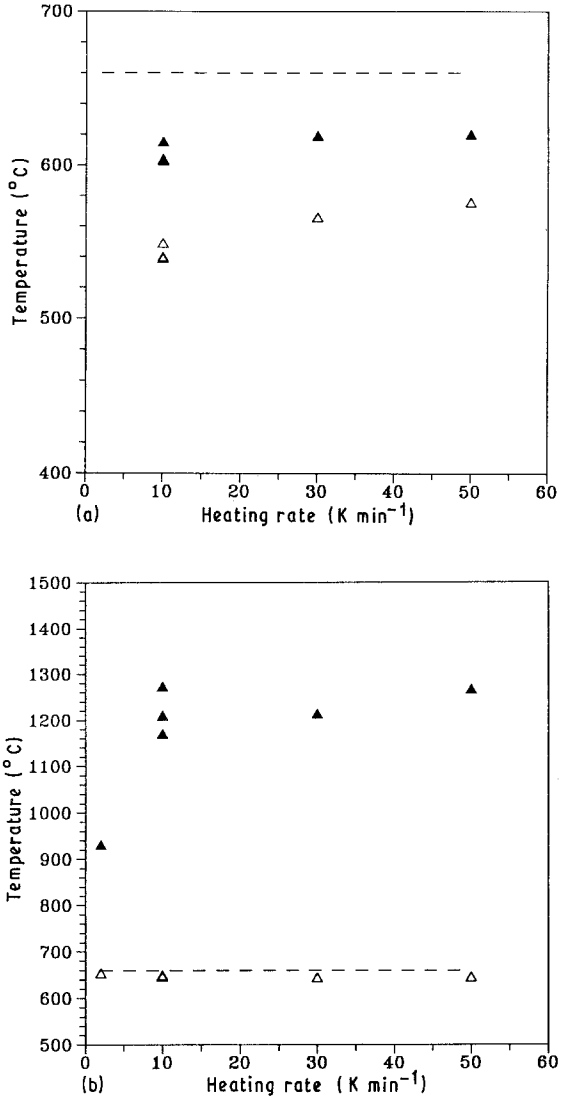

Figure 7 Effect of heating rate on (△) ignition and (▲) combustion temperatures of (a) the first peak and (b) the second peak in the Ti + 3Al = $TiAl_3$ reaction; (– – –) melting point of Al.

different heating rates (Fig. 14) and the products exhibited evenly distributed porosities (Fig. 12). Another interesting phenomenon, as can be seen from Figs 6, 13 and 14, is that green density has insignificant effect on the density of the reacted products for all of the reactions. The XRD results are summarized in Table III.

3.2. Effect of composition

As stated earlier, there is no significant change in either ignition or combustion temperature of either peak as a function of composition, but the relative densities of the reacted products decreased with the increase of aluminium content in spite of the fact that the relative densities of the green pellets were similar. Fig. 15 shows the relative density versus composition plot for a heating rate of 10 K min^{-1}. It was found that both the Ti_3Al and Ti–27.3 wt % Al (TiAl + Ti_3Al) specimens maintained their cylindrical shape after reaction, whereas the TiAl and $TiAl_3$ pellets were bloated, especially the latter. These facts clearly indicate that it is aluminium rather than titanium particles that are responsible for the bloating.

3.3. The role of oxide formation

Though the reaction was carried out in an argon atmosphere, it was still found that the weight of the product increased by about 1% after reaction. By differential thermal analysis (DTA) and thermogravimetric analysis (TGA) of TiAl reaction using a rate of 10 K min^{-1}, it was found that a continuous weight gain occurred throughout the whole heating process. This could be attributed to the oxygen impurity in the ultra-high purity argon, since both the titanium and aluminium are easily oxidized. In this case, the weight gain from oxidizing titanium might be larger than that from oxidizing aluminium since aluminium particles already have an oxide coating.

Like the situation of synthesizing Ti–Ni intermetallics [10, 11], the oxidization process also influences the reaction greatly if the process occurs at a fast rate. Fig. 16 shows the edge area of an SEM photomicrograph of a sample reacted by the oxygen-assisted reaction (oxide formation) at a heating rate of 10 K min^{-1}. Compared with Fig. 5a, the edge area in Fig. 16 appears much denser than the inner area as if a liquid product had formed, i.e. the combustion temperature exceeded the melting point of the TiAl compound. Indeed, the combustion temperature recorded was 1461 °C which is the melting point of the TiAl compound. This enhanced exothermic phenomenon is believed to originate from the oxidation of elemental aluminium and/or titanium, which inputs extra heat to the system similar to the situation found in the Ti–Ni system [10, 11]. However, the heating rate must be sufficiently rapid in order for the heat of oxidation to trigger the main reaction rather than to dissipate into the surroundings [10, 11].

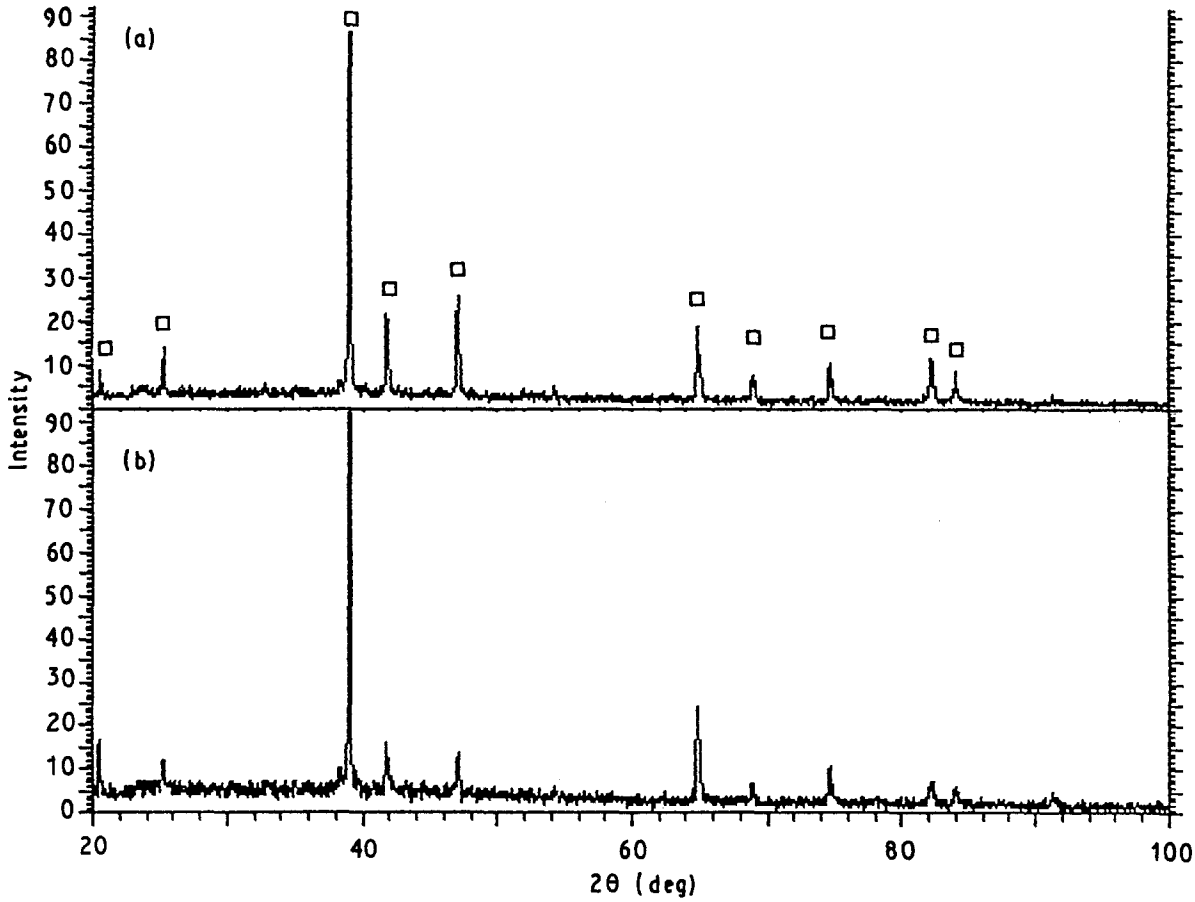

Figure 8 XRD patterns of the $TiAl_3$ product under different heating rates: $\dot{T}$ = (a) 2 and (b) 50 K min^{-1}. (●) TiAl, (□) $TiAl_3$, (■) Ti_3Al, (▽) Ti.

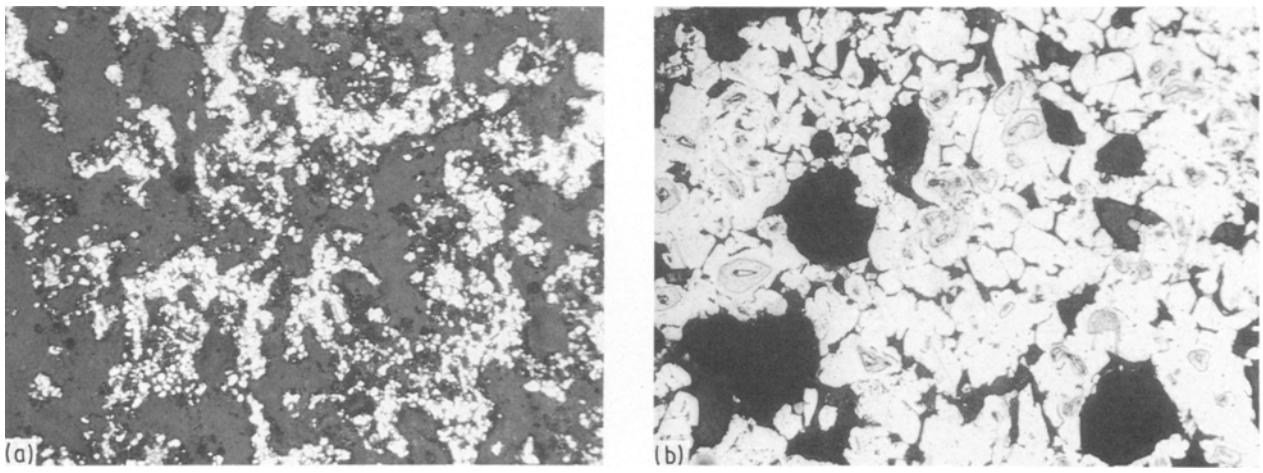

Figure 9 Optical micrographs of the $TiAl_3$ product under different heating rates: $\dot{T}$ = (a) 2 and (b) 50 K min^{-1} (×150).

4. Discussion

4.1. Origin of the first peak

In combustion synthesis studies of the Ni–Al system, Philpot *et al.* [9] found that two exothermic peaks occurred for some compositions under certain heating rates. They concluded that both peaks were due to solid–solid reactions between the two elements. In order to determine the reaction mechanism of the first peak in the present work, three samples were heated up to different temperatures marked a, b and c in Fig. 2, using a heating rate of 10 K min^{-1}. These samples were then analysed by XRD (Table II) and examined by SEM. Surprisingly, no evidence of compound formation was found either before or just after the first exothermic peak (points a and b in Fig. 2, respectively). Actually, the first traces of compound observed were not TiAl as expected but $TiAl_3$ after the temperature of the sample surpassed the melting point of

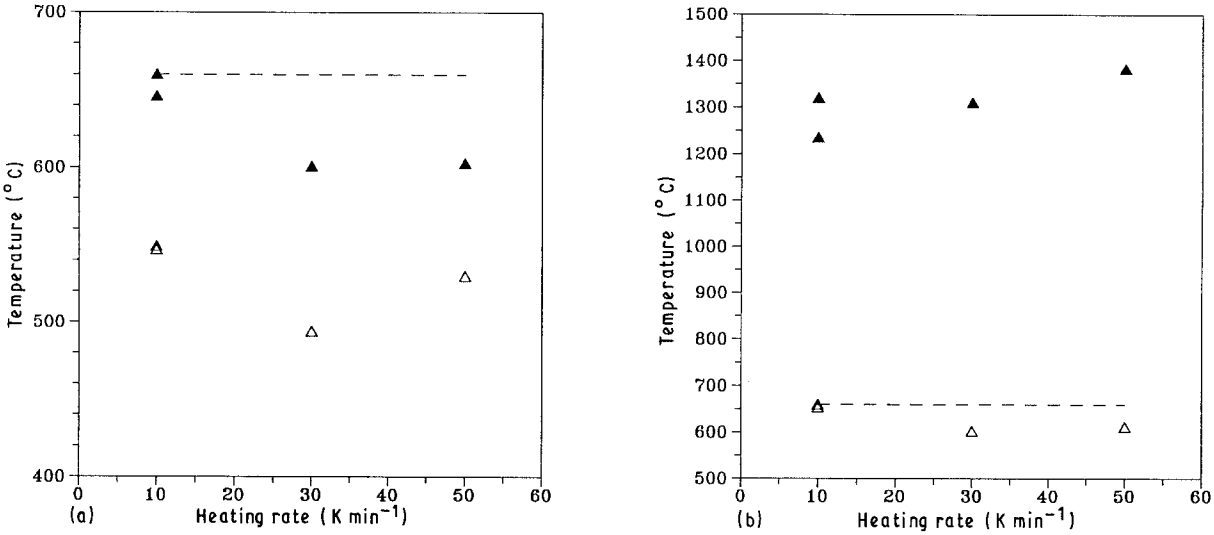

Figure 10 Effect of heating rate on (△) ignition and (▲) combustion temperatures of (a) the first peak and (b) the second peak in the $3Ti + Al = Ti_3Al$ reaction; (– – –) melting point of Al.

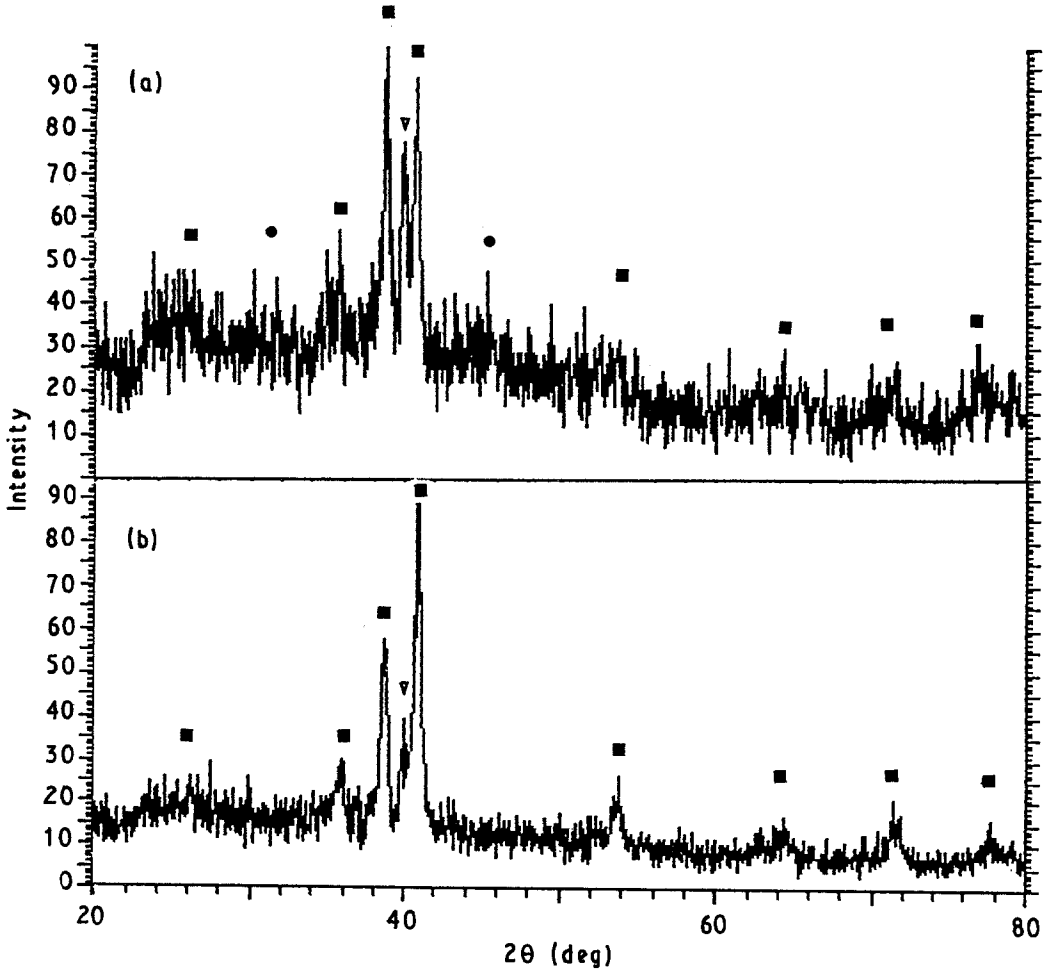

Figure 11 XRD patterns of the Ti_3Al product under different heating rates: $\dot{T}$ = (a) 10 and (b) 50 K min^{-1}. (●) TiAl, (□) $TiAl_3$, (■) Ti_3Al, (▽) Ti.

aluminium (point c in Fig. 2) as shown in Fig. 17. This phase was found by SEM at the boundary between aluminium and titanium particles. These facts clearly show that the $TiAl_3$ compound was formed only after the melting point of aluminium and not during the first exothermic peak.

Therefore, the first peak was not due to solid–solid reaction as in the case of Ni–Al. However, on checking the density changes for different reactions shown in Figs 6 and 13–15 where a lower-density product always resulted for higher aluminium compounds, it can be concluded that the first peak must be related to the

TABLE III Summary of XRD results

Compound	Reaction parameters		Phases detected[a]				
	$\dot{T}$ (K min^{-1})	T_c (°C)	TiAl	Ti_3Al	$TiAl_3$	Ti	Al
TiAl	10	1383	p	m	m	t	n
	1	1077	m	p	m	t	t
	50	1313	p	m	t	t	n
	After the melting of Al[b]		n	n	t	p	p
	Temp. just reaches T_m(Al)[c]		n	n	n	p	p
$TiAl_3$	10	931	n	n	p	t	n
	50	1267	n	n	p	t	t
Ti_3Al	10	1235	m	p	t	m	n
	50	1383	t	p	t	m	n

[a] p = predominant, m = medium amount, t = traces, n = not detected.
[b] Heated to point c in Fig. 2.
[c] Heated to point b in Fig. 2.

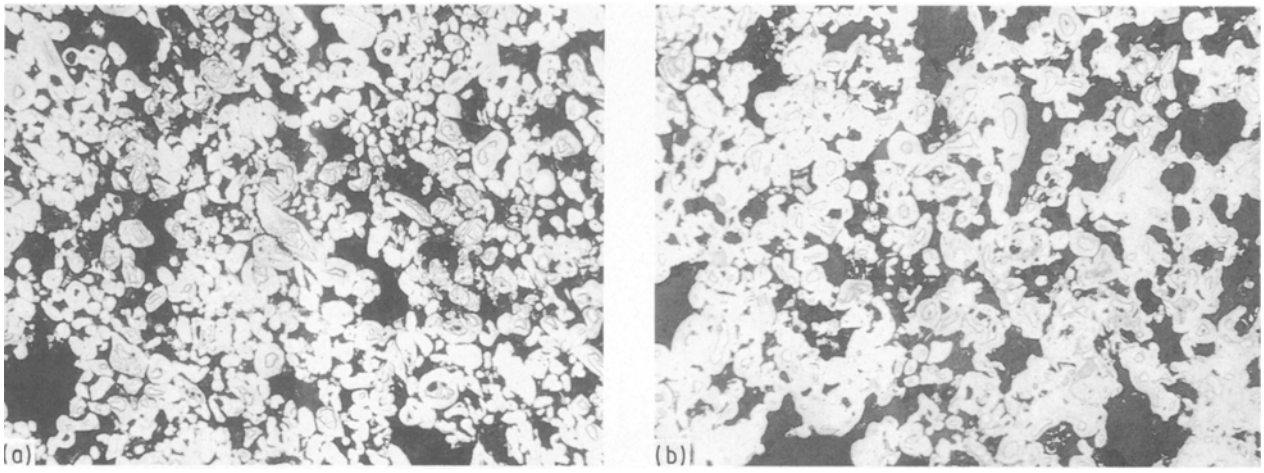

Figure 12 Optical micrographs of the Ti_3Al product under different heating rates: $\dot{T}$ = (a) 10 and (b) 50 K min^{-1} (× 150).

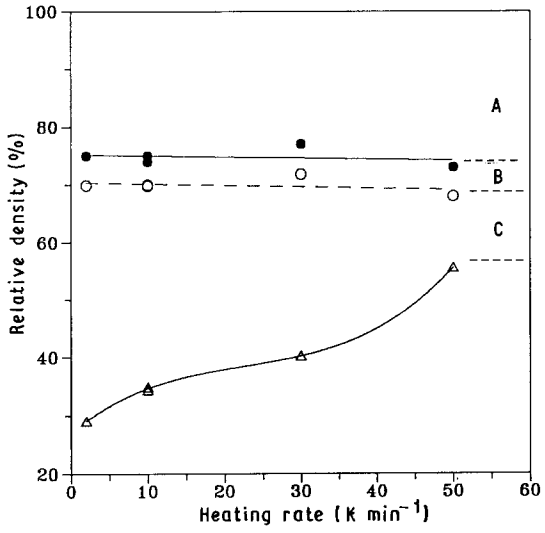

Figure 13 Effect of heating rate on the density changes of Ti + 3Al = $TiAl_3$ reaction; regions A, B, C represent three kinds of porosity. (○) 0.932 relative green density, (●) relative green density, (△) relative product density.

aluminium particles. It is proposed here that the peak originates from the decomposition of hydrated aluminium oxide. The elemental powders physically absorb water (moisture), hydrogen and oxygen, and form chemically hydrated aluminium oxides ($Al_2O_3 \cdot 3H_2O$ or $Al_2O_3 \cdot H_2O$). During heating, most of the physically absorbed water would evaporate above 100 °C. Between the temperatures 530 and 550 °C, the dissociation of the hydrated aluminium oxide takes place as follows [13]:

$$Al_2O_3 \cdot 3H_2O = Al_2O_3 + 3H_2O \quad (1)$$

$$Al_2O_3 \cdot H_2O = Al_2O_3 + H_2O \quad (2)$$

The water vapour released by Reactions 1 and 2 then reacts with elemental titanium and aluminium to form oxides plus hydrogen gas as follows:

$$3H_2O + 2Al = Al_2O_3 + 3H_2 \quad (3)$$

$$H_2O + Ti = TiO \text{ (or } TiO_2) + H_2 \quad (4)$$

Reactions 1 to 4 are together responsible for the first peak. On the other hand, since the aluminium particles are always coated with an alumina layer which protects the aluminium particle from being further oxidized, Reaction 4 may play a more important role than Reaction 3 does.

It was also found that the gases released after the reaction associated with the first peak (H_2O and H_2)

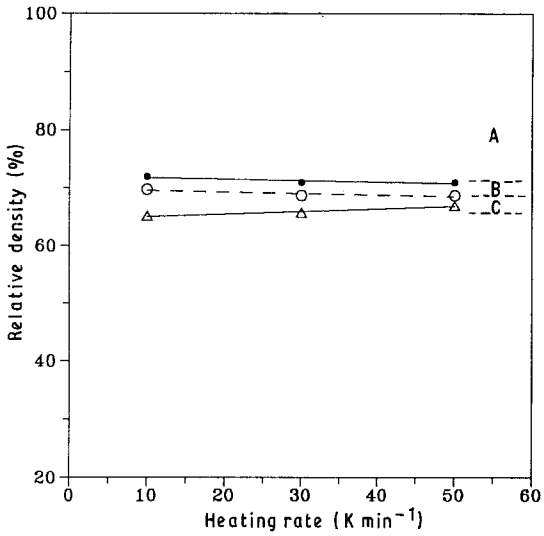

Figure 14 Effect of heating rate on the density changes of $3Ti + Al = Ti_3Al$ reaction; regions A, B, C represent three kinds of porosity. (○) 0.969 relative green density, (●) relative green density, (△) relative product density.

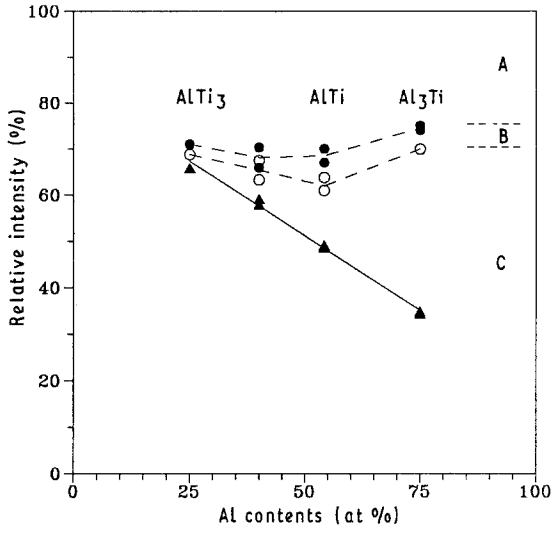

Figure 15 Relative densities of the reactants and products under different aluminium composition: (○) $C \times$ relative green density, (●) relative green density, (▲) relative product density.

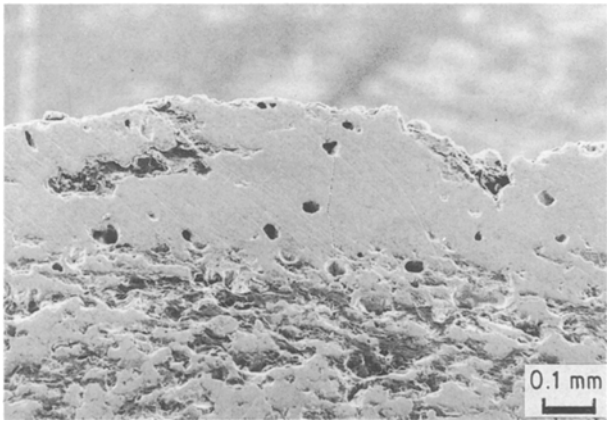

Figure 16 SEM photograph of the edge area of TiAl compound produced at a heating rate of 10 K min^{-1} and assisted by oxidation.

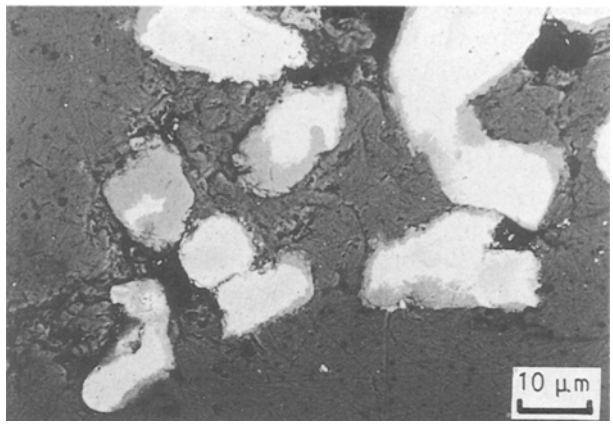

Figure 17 SEM photograph of TiAl pellet heated after the melting of aluminium but before the main reaction, showing $TiAl_3$ compound formation between the titanium and aluminium particles.

have difficulty in escaping. They are trapped in the pellet and can only be released after the violent second peak main reaction since the shape of the pellet did not change when the sample was heated to point c, i.e. just before the main reaction.

Reactions 1 and 2 are irreversible. Therefore, if the pellet is heated up after the first but before the second peak and cooled down, then heated up again, there should be no first peak. Such an experiment on a $TiAl_3$ pellet using a heating rate of 10 K min^{-1} confirmed this hypothesis.

Hence, the lower density for the higher aluminium content (Fig. 15) reaction is due to increased gases released by the dissociation represented by Equations 1 and 2. The fact that the product density increased with the increase of heating rate as shown in Figs 6 and 13 for the TiAl and $TiAl_3$ reactions also derives from the same source, i.e. the dissociation process may occur fast and a portion of released gases escapes from the pellet before the main reaction. The higher heating rate may also result in a higher combustion temperature which increases the density as well. On the other hand, the effect of dissociation of hydrated aluminium oxides on the product density is too weak to detect for the Ti_3Al reaction (Fig. 14) since the aluminium content is relatively small.

4.2. Reaction mechanism

Figs 3b, 7b and 10b indicate that the reaction mechanisms are different under different heating rates, i.e. a liquid (Al)–solid (Ti) reaction at lower heating rates and a solid–solid reaction for higher heating rates. This difference is probably related to Equations 1–4 as well. Under a lower rate, the exothermic process represented by Equations 1 to 4 occurred more slowly and part or all of the heat released by the reaction was dissipated. The reaction between titanium and aluminium will not be initiated until the temperature reaches the melting point of aluminium. At a higher heating rate, more heat released by Reactions 1 to 4 is retained by the system so that the main reaction can be triggered at a lower temperature.

The consequence of the above process explains the results shown in Fig. 4 and Table III, where a mixture of phases results for heating rates below 10 K min^{-1} whereas a single-phase product forms at a heating rate of 50 K min^{-1} and above. Under a lower heating rate, the combustion reaction was preceded by the melting of aluminium which enhances the reaction since the liquid aluminium has a much higher reactivity than solid aluminium. Hence, once the melting point of aluminium had been reached, the liquid aluminium would surround the titanium particle and the reaction, most likely the formation of $TiAl_3$ as shown in Fig. 17, would start at contacting surfaces of dissimilar particles. This compound formation would in turn supply extra heat to the system and further increase the reaction rate until the system accumulated sufficient heat to trigger the main reaction throughout. Since some $TiAl_3$ phase was already being formed before the main reaction (at the temperature between the melting point of aluminium and the ignition temperature), the final product would have to contain the same moles of Ti_3Al compounds for stoichiometric balance reasons. On the other hand, at heating rates higher than 50 K min^{-1}, since the ignition temperature is lower than the melting point of aluminium (Figs 3b, 7b and 10b) there is no $TiAl_3$ compound formation prior to the major reaction and therefore the reacted product should be solely TiAl phase. In this case the second phase was probably from the mixing of inhomogeneous reactant powders.

The same explanation may apply to the reaction of other compounds in this study.

4.3. Density change

As pointed out by Munir and Wang [14], the porosity in the reacted products has four possible sources. They are: (i) existing porosity in the pressed pellet, (ii) differences in molar volume between reactants and product, (iii) gas evolution during reaction, and (iv) thermal migration due to a high temperature gradient in the combustion mode. It is believed that the last one is less important in the present work compared with the other three. The first one is the main contribution in this work since the green pellets pressed were between 70 and 80% of theoretical density. If we suppose that there is no weight change after reaction, then we have

$$\nu_p = \left(\frac{\rho_r}{\rho_p}\right)\nu_r\left(\frac{V_r}{V_p}\right) = C\left(\frac{V_r}{V_p}\right)\nu_r \quad (\%) \quad (5)$$

where ν, ρ and V are relative density (percentage of theoretical density), theoretical density and volume, respectively. Subscripts r and p denote reactant and product, respectively. C is a constant, i.e. the ratio of theoretical densities of the reactants and products, or the ratio of the molar volume of the reactants and products which is 0.911 for TiAl, 0.932 for $TiAl_3$ and 0.969 for Ti_3Al.

If there is no dimensional change after reaction, then the relative product density would be $0.911\,\nu_r$ for TiAl which means there is 8.9% porosity attributable to the molar volume difference between Ti + Al and TiAl. If $\nu_p > 0.911\nu_r$, $V_p < V_r$, the product densifies (or shrinkage occurs). If the opposite is true, then product swelling occurs. Therefore, Equation 5 can probably be used as a criterion to determine whether densification or swelling occurs after reaction.

It is obvious from Fig. 15 that the samples swelled for all of the compounds studied. According to the above argument, the porosity shown in Figs 6 and 13–15 can then be divided into three sources: fraction A is from the porosity existing in the reactants, fraction B is from molar volume changes between reactants and products. Fraction C is due to the outgassing of trapped H_2O and H_2 released by Reactions 1 and 2.

5. Conclusions

In synthesizing the Ti–Al compounds, the heating rate is a very important parameter which greatly influences the overall reaction mechanism and the density of the product. A higher heating rate results in not only a more densified but also a more homogeneous product. Under lower heating rates, a liquid (Al)–solid (Ti) reaction mechanism occurs while a solid–solid reaction mechanism is predominant for higher heating rates. On the other hand, the combustion temperatures do not change greatly as a function of heating rate or composition. A more sensitive temperature measurement apparatus may detect some influence in variation of these parameters. The porosity of the reacted product has been attributed to three sources.

References

1. Z. A. MUNIR and U. ANSELMI-TAMBURINI, *Mater. Sci. Rep.* **3** (1989) 277.
2. T. B. MASSALSKI *et al.* (eds), "Binary Alloy Phase Diagrams", Vol. 1 (American Society for Metals, 1986), p. 175.
3. A. G. MERZHANOV and I. P. BOROVINSKAYA, *Dokl. Chem.* **204** (1972) 429.
4. Yu M. MAKSIMOV, A. T. PAK, G. B. LAVRENCHUK, Yu S. NAIBORENDENKO and A. G. MERZHANOV, *Comb. Explos. Shock Waves* **15** (1979) 415.
5. Yu S. NAIBORODENKO, G. V. LAVRENCHUK and V. M. FILATOV, *Sov. Powd. Metall. Met. Ceram.* **21** (1982) 909.
6. W. R. WRZESINSKI and J. C. RAWERS, *J. Mater. Sci. Lett.* **9** (1990) 432.
7. Y. KAIEDA, M. NAKAMURA, M. OTAGUCHI and N. OGURO, in Proceedings of 1st US–Japanese Workshop on Combustion Synthesis, edited by Y. Kaieda and J. B. Holt (National Research Institute for Metals, Tokyo, 1990) p. 207.
8. P. H. SHINGU, K. N. ISHIBARA, F. GHONOME, T. HAYAKAWA, M. ABE and K. TAGUCHI, *ibid.* p. 65.
9. K. A. PHILPOT, Z. A. MUNIR and J. B. HOLT, *J. Mater. Sci.* **22** (1987) 159.
10. H. C. YI and J. J. MOORE, *J. Mater. Sci.* **24** (1989) 3449.
11. *Idem, ibid.* **24** (1989) 3456.
12. L. L. WANG, Z. A. MUNIR and J. B. HOLT, *Met. Trans.* **21B** (1990) 567.
13. A. LAWLEY, *JOM* **42**(4) (1990) 12.
14. Z. A. MUNIR and L. L. WANG, in Proceedings of 1st US–Japanese Workshop on Combustion Synthesis, edited by Y. Kaieda and J. B. Holt (National Research Institute for Metals, Tokyo, 1990) p. 123.

Received 13 December 1991
and accepted 2 June 1992